IEEE Journal of Translational Engineering in Health and Medicine

Received 20 April 2018; revised 5 July 2018 and 27 August 2018; accepted 29 August 2018.
Date of publication 11 October 2018; date of current version 25 October 2018.

Digital Object Identifier 10.1109/JTEHM.2018.2868671

A New Method for Diaphragmatic Maximum Relaxation Rate Ultrasonographic Measurement in the Assessment of Patients With Diaphragmatic Dysfunction

CHRISTOS P. LOIZOU[1], (Senior Member, IEEE), DIMITRIOS MATAMIS[2], GIORGOS MINAS[3], THEODOROS KYPRIANOU[3], CHRISTAKIS D. LOIZOU[4], ELENI SOILEMEZI[2], ENTELA KOTCO[2], and CONSTANTINOS S. PATTICHIS[5], (Fellow, IEEE)

[1]Department of Electrical Engineering, Computer Engineering and Informatics, Cyprus University of Technology, 3036 Limassol, Cyprus
[2]Intensive Care Unit, Papageorgiou General Hospital, 546 46 Thessaloniki, Greece
[3]Intensive Care Unit, Nicosia General Hospital, 2029 Nicosia, Cyprus
[4]Department of Biomedical Engineering, Imperial College London, London SW7 2AZ, U.K.
[5]Department of Computer Science, University of Cyprus, 1678 Nicosia, Cyprus

CORRESPONDING AUTHOR: C. P. Loizou (christos.loizou@cut.ac.cy)

This work was supported by the H2020-WIDESPREAD04-2017-Teaming Phase 1, Integrated Precision Medicine Technologies (IPMT), under Grant 763781.

ABSTRACT Measurements of ultrasound diaphragmatic motion, amplitude, force, and velocity of contraction may provide important and essential information about diaphragmatic fatigue, weakness, or paralysis. In this paper, we propose and evaluate a semi-automated analysis system for measuring the diaphragmatic motion and estimating the maximum relaxation rate (MRR_SAUS) from ultrasound M-mode images of the diaphragmatic muscle. The system was evaluated on 27 M-mode ultrasound images of the diaphragmatic muscle [20 with no resistance (NRES) and 7 with resistance (RES)]. We computed semi-automated ultrasound MRR measurements on all NRES/RES images, using the proposed system (MRR_SAUS $=$ $3.94 \pm 0.91/4.98 \pm 1.98$ [1/s]), and compared them with the manual measurements made by a clinical expert (MRR_MUS $= 2.36 \pm 1.19/5.8 \pm 2.1$ [1/s],) and those made by a reference manual method (MRR_MB $= 3.93 \pm 0.89/3.73 \pm 0.52$ [1/sec], performed manually with the Biopac system. MRR_SAUS and MRR_MB measurements were not statistically significantly different for NRES and RES subjects but were significantly different with the MRR-MUS measurements made by the clinical expert. It is anticipated that the proposed system might be used in the future in the clinical practice in the assessment and follow up of patients with diaphragmatic weakness or paralysis. It may thus potentially help to understand post-operative pulmonary dysfunction or weaning failure from mechanical ventilation. Further validation and additional experimentation in a larger sample of images and different patient groups is required for further validating the proposed system.

INDEX TERMS Diaphragmatic muscle, diaphragmatic motion analysis, diaphragmatic ultrasound, maximum relaxation rate (MRR).

I. INTRODUCTION

The dysfunction of the diaphragm, which is the main respiratory muscle for quiet breathing (normal breathing state that requires no control or assistance of any type), contributing up to 70% to resting lung ventilation, may induce respiratory complications and can prolong the duration of mechanical ventilation [1]–[5]. Early diagnosis of diaphragmatic dysfunction is important, because diaphragmatic paralysis may be amenable to therapeutic strategies and may require adapted and prolonged ventilatory support. Therefore, the need for the assessment of diaphragm function arises in many clinical situations. An early index for the evaluation

IEEE Journal of Translational Engineering in Health and Medicine

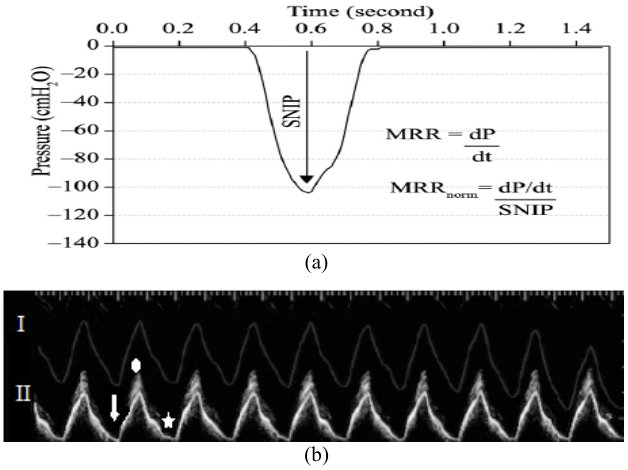

FIGURE 1. **(a) Equations used in the calculation of the MRR of the Esophageal pressure (MMR_ES). Reproduced from [2]. (b) Inverted esophageal pressure (I) generated by the Biopac®system (reference method) and its corresponding diaphragmatic motion (M-mode) (II) acquired by ultrasound, from a female subject at the age of 45 with no-resistance (NRES) in the esophageal muscle. ↓: End of expiration (beginning of the diaphragmatic contraction), O: End of inspiration (end of diaphragmatic contraction), ∗: End of relaxation.**

of the diaphragmatic fatigue is the maximum relaxation rate (MRR) of the esophageal pressure (MRR_ES) which is depicted in Fig. 1a. MRR_ES has been used as a predictor of weaning failure [4], [5]; however, the invasive nature of the measurement method has impeded its wide clinical use [2]. In order to estimate the MRR_ES, the slope of a tangent, drawn at the steepest part of the esophageal pressure graph (see also Fig. 1a), is divided by the value of the peak pressure [3]–[5]. Diaphragmatic motion can also be monitored by ultrasound video, from which an M-mode image (see Fig. 1b) may be generated [6]. An M-mode image of the diaphragm can evaluate the diaphragms' displacement and kinetics, which can assist the clinical expert in the evaluation and assessment of the fatigue of the diaphragm [6]. Abnormalities of the MRR may indicate impaired contractile performance [6].

The method initially described for the measurement of the MRR involves passing a specially designed catheter in the lower third of the esophagus for measurement of the esophageal pressure [4]–[8]. The measuring system requires appropriate calibration and performance of specific tests to assure proper position and reliable measurements [6]. The maximal rate of the relaxation part of the esophageal pressure curve is taken as the diaphragmatic MRR [4], [5]. However, in total, the technique is cumbersome and invasive in nature and due to some technical limitations, measurement of diaphragmatic MRR was mainly used for research purposes rather than in everyday clinical practice. Meanwhile, ultrasonography has become increasingly available in ICUs worldwide; soon it was discovered that diaphragmatic motion is easily and reliably recorded using M-mode sonography. Assessment of the distance, velocity and duration of diaphragmatic motion became subsequently readily available, allowing for direct measurement of the contraction and, of what is of major clinical interest, relaxation rate of the diaphragm; however, the examiner has to decide which part of the relaxation M-mode displacement curve represents the initial, steepest part (see also Fig. 2f) where measurement of the relaxation rate will be performed.

Few other researchers have investigated in the past the diaphragmatic fatigue and dysfunction from ultrasound images or videos [6]–[9]. In [6] diaphragmatic dysfunction was diagnosed by M-mode ultrasonography in ultrasound M-mode images respectively. In [7], diaphragmatic motion using M-mode analysis was correlated with pulmonary function in stroke patients. Boussuges *et al.* [8], investigated the diaphragmatic motion by using M-mode ultrasonography and extracted the normal values of the excursion of the diaphragmatic muscle. In the above studies, the use of ultrasound imaging or video for the diaphragmatic function in clinical applications was found to be very useful. Furthermore, in [9] three-dimensional reconstructions obtained with spiral computed tomography were used to measure total diaphragm length and surface area, where a reduction of the diaphragmatic area was observed in subjects with obstructive pulmonary disease.

The objective of the present study was to propose a semi-automated system to compute maximum relaxion rate (MRR_SAUS) of the diaphragm using ultrasound M-mode images and extract the displacement curve as well as quantitative parameters (see also Fig. 2). These parameters will be able to assist the clinician in the noninvasive evaluation of the diaphragmatic muscle fatigue and aid in the proper decision of medical treatment. To the best of our knowledge, there are no other studies reported in the literature (with the exception of [10] applied only in three healthy volunteers by our group), investigating the diaphragmatic MRR_SAUS using ultrasound M-mode images of the diaphragmatic muscle. Moreover, in [11], a system for the quantitative analysis of the ultrasonic diaphragmatic motion was introduced, which was based on motion analysis of the diaphragmatic ultrasound videos.

The proposed semi-automated system constitutes an easy method to accurately locate and calculate diaphragmatic MRR. Additionally, being user friendly, users may be able to familiarize them self's easily with the system. The time line for the development of the proposed system will depend on the readiness of the intensive care units (ICU's) worldwide to implement and apply the proposed system in the current clinical practice. The noninvasive evaluation of the diaphragmatic muscle will then be possible, and one would expect a rapid implementation of the proposed method, since current evaluation of the calculation of diaphragmatic MRR is mainly performed using a cumbersome, invasive method, i.e. via inserting an esophageal catheter [6].

II. METHODOLOGY

Figure 2 illustrates the steps followed for the measurement of the diaphragmatic MRR_SAUS index, from an M-mode

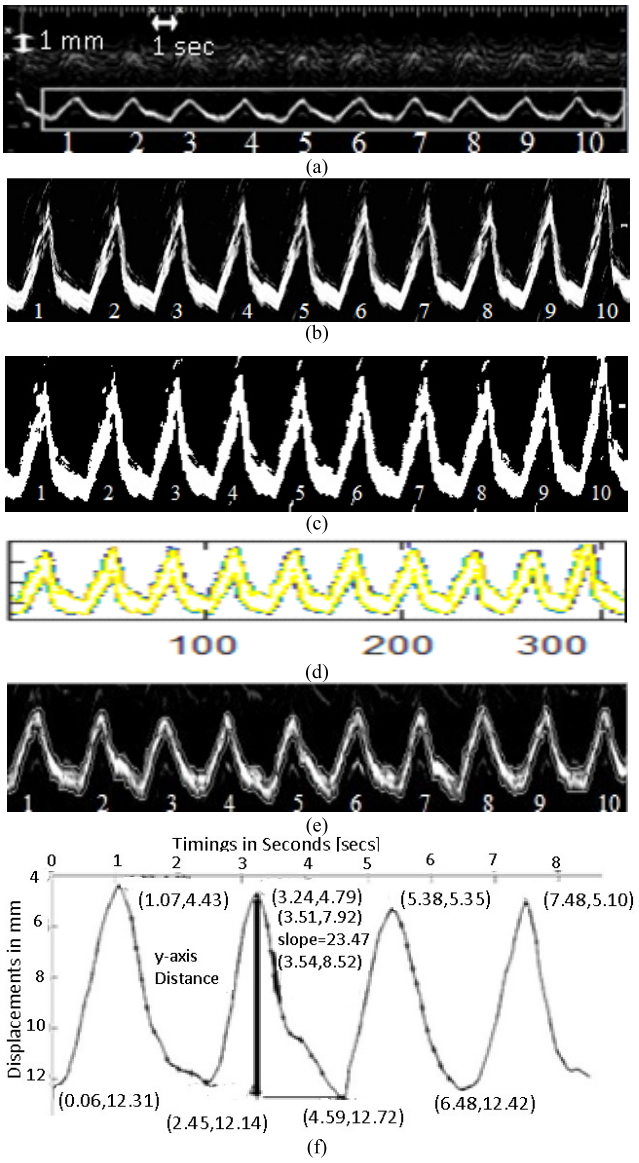

FIGURE 2. **Illustration of the steps followed for the semi-automated measurement of the diaphragmatic MRR_SAUS index. (a) Initial ultrasound M-mode image of the diaphragmatic motion with the selected rectangular ROI and the calibration points placed manually by the user of the system for ten breathing cycles. The ultrasound M-mode image was acquired from a male subject at the age of 45 without the use of resistance during breathing (NRES). (b) Diaphragmatic ultrasound motion curve after image normalization and despeckle filtering. (c) Binary image from (c). (d) Extraction of the upper and lower boundaries of the diaphragmatic motion curve. (e) Final upper and lower boundaries overlaid on the grayscale diaphragmatic ultrasound image. (f) Upper smoothed graph of the diaphragmatic displacement for the first four breaths with absolute maximum [4.59 mm, 12.72 mm] and minimum [3.24 mm, 4.79 mm] values and the steepest slope [23.47 mm/sec], at the coordinates [3.51 sec, 7.92 mm] and [3.54 sec, 8.52 mm]. Absolute maximum and minimum distance (diaphragmatic displacement): 12.72-4.79 = 7.93 mm, Cycle duration = 2.4 secs; MRR_SAUS = 3.92 1/sec.**

ultrasound diaphragmatic image. Figure 3 summarizes in detail the steps followed in the form of a flow diagram, where it is shown how the diaphragmatic motion diagram, the final contracting, and relaxing diaphragmatic states, as well as the MRR_SAUS index value of the diaphragm were estimated. These will be explained in the following subsections.

Step 1: Acquire and load the M-Mode diaphragmatic ultrasound image for analysis.
Step 2: Apply image intensity normalization [12]. Manually calibrate the M-mode image by selecting two consecutive points on the x- and y-axis (see left top corner of Fig. 2a), that corresponds to 1 sec and 1mm respectively. Manually remove erroneous edges.
Step 3: Manually identify the relaxation and contraction points of the diaphragm, the MRR_MUS, the slope, the excursion, the cycle duration, and the inspiration time [6].
Step 4: Manually select a rectangular region of interest (ROI) (see also Fig. 2a), in order to define the region, where the M-mode image, the displacement of the diaphragm and the measurements will be estimated by the proposed method.
Step 5: Apply DsFlsmv despeckle filtering [13] on the selected ROI (see also Fig. 2b).
Step 6: Convert the M-Mode image to binary and extract the edges of the diaphragmatic diagram. Link the edges to form an initial boundary (see also Fig. 2c).
Step 7: Fit the diaphragmatic boundaries to a snake's segmentation algorithm [15] and extract the final diaphragmatic upper and lower boundaries (see also Fig. 2d).
Step 8: Estimate the upper boundary of the diaphragmatic motion diagram (see also Fig. 2d) to compute the excursion, cycle duration, inspiration time, total time, slope, relaxation rate, steepest slope and MRR_SAUS. Sample the upper boundary in equal equidistant segments (see Fig. 2f).
Step 9: Compute the steepest slope according to (3) and the MRR_SAUS for each descending (relaxation) diaphragmatic curve and each equidistant segment.
Step 10: Compute and display the evaluation metrics between the automated and manual displacement and timing measurements.

FIGURE 3. **Steps followed in the measurement of ultrasonic diaphragmatic motion.**

A. ACQUIRING M-MODE ULTRASOUND DIAPHRAGMATIC IMAGES

A total of 27 M-mode ultrasound images of the diaphragmatic muscle from individual subjects (20 male, 7 female) (COMB) at the age of 41.6 $\pm$ 4.4 with abnormal diaphragmatic function were recorded during quiet breathing, using the Philips HD15 U/S scanner at the ICU of the Papageorgiou Hospital in Thessaloniki, Greece. In seven patients a resistive device was added (RES) in the breathing circuit for a few breathing efforts, while in the rest of the patients breathing was without resistance (NRES).

All subjects were examined during a routine diagnostic procedure and a written informed consent was obtained according to the instructions of the local ethics committee, while all personal data were kept confidential.

IEEE Journal of Translational Engineering in Health and Medicine

For each acquired M-mode ultrasound image, the calibration was made by selecting two consecutive points on the x-axis (see left top corner of Fig. 2a), that corresponds to 1 sec and two points on the y-axis that correspond to 1 mm. Points were manually selected by the user of the proposed system, in order to extract reliable and consistent measurements (see also Fig. 3, step 2-step 4). The calibration was made after image normalization (see subsection II.B) Erroneous edges or readings that were possibly produced during the image acquisition process can be manually removed from the user of the system by using the mouse (see Fig. 3, step 2).

A highly experienced ICU specialist, with more than 30 years of experience (coauthor D. Matamis), manually identified (after image normalization, see subsection II.B) the relaxation and contraction points of the diaphragm from the acquired ultrasound M-mode images, as well as manually measured the MRR_MUS of the diaphragmatic curve, the slope, the excursion, the cycle duration, and the inspiration time [6] (see also Fig. 3, step 3). The ICU specialist additionally measured the maximum relaxation rate (MRR_MB) using the reference Biopac®system [6].

The ICU specialist manually calibrated the M-mode images and selected an ROI. On the diaphragmatic M-mode ultrasound image (see Fig. 2a), a rectangular region of interest (ROI) was manually selected (see also Fig. 2a and Fig. 3, step 4) by the user, in order to define the region, where the M-mode image, the displacement of the diaphragm and the measurements will be estimated.

B. IMAGE NORMALIZATION AND DESPECKLE FILTERING

All images were intensity resolution-normalized depending on the calibration of the image as proposed in [12] by selecting the darkest and brightest area in the image (see also Fig. 3, step 2). During the normalization procedure, a small homogeneous area in the darkest area of the image was selected and the grayscale median value of this area was estimated, which was in the range from 3-9. In the same manner, a small homogeneous area in the brighter was selected and the grayscale median of this area was also estimated, which was in the range of 190-210. Care was taken during the normalization procedure, so that an area with the above characteristics would be selected [13]. Algebraic (linear) scaling of the image was manually performed by linearly adjusting the image based on the dark and bright values selected above. The result of this is that the intensity of the gray level values on the image ranged from 0-255. Thus, the brightness of all pixels in the image was readjusted according to the linear scale defined by selecting the two reference regions [12]. The normalization procedure applied is a well-accepted standardization method used widely and it improves image compatibility by reducing the variability introduced by different gain settings, different operators, different equipment, and facilitates ultrasound tissue comparability. This was also carried out in order to overcome the small variations in the number of pixels per mm of the image depth and in order to maintain uniformity in the digital image spatial resolution.

For speckle reduction, which was applied after image normalization, on the selected ROI (see Fig. 3, step 5), the filter DsFlsmv (despeckle filter linear scaling mean variance) was applied to the ROI in each M-Mode ultrasound image prior to measuring the MRR_SAUS (see also Step 4, in Fig. 3 and Fig. 2b)). The filters of this type utilize first order statistics such as the variance and the mean of a pixel neighborhood and may be described with a multiplicative noise model [13], [14] by the following equation:

$$f_{i,j} = \bar{g} + k_{i,j}\left(g_{i,j} - \bar{g}\right) \tag{1}$$

where $f_{i,j}$, is the estimated noise-free pixel value, $g_{i,j}$, is the noisy pixel value in the moving window, $\bar{g}$, is the local mean value of an $N_{1x}N_2$ region surrounding and including pixel $g_{i,j}$, $k_{i,j}$ is a weighting factor, with $k \in [0, 1]$, and i, j are the pixel coordinates. The factor $k_{i,}$, is a function of the local statistics in a moving window and is defined [13], [14] as:

$$k_{i,j} = \frac{(1 - \bar{g}^2\sigma^2)}{\sigma^2 + \sigma_n^2} \tag{2}$$

The values σ^2 and σ_n^2 represent the variance in the moving window and the variance of the noise in the whole M-Mode ultrasound image respectively. The moving window size for the despeckle filter DsFlsmv was 5x5 and the number of iterations applied to each image was one, where a complete description of the filter and its parameters can be found in [13] and [14].

C. M-MODE IMAGE ANALYSIS

The M-mode ultrasound images were further processed using the Matlab® Simulink Software. First, all the images were converted to binary (see Fig. 2c), using the im2bw function in Matlab® R 2015b, and morphological operators (closing and opening using a cross structuring element of size 3x3) were applied to smooth the edges of the ultrasound diaphragmatic muscle. The edges were then extracted using an appropriate threshold for the image binarization, which was automatically estimated using the graythresh function in Matlab® R 2015b (see Fig. 3, step 6 and Fig. 2c). The image edges representing the diaphragm, were then linked together and then sampled, to produce a parameterized contour with x- and y-coordinates (see Fig. 2d). This contour was then inputted to a snake's segmentation algorithm, which is a modification of the Williams & Shah snake's algorithm as presented in [15] (see Fig. 3, step 7). The snake was applied to every binary image and deformed in order to extract the exact final boundaries of the diaphragmatic motion diagram (see Fig. 2e and Fig. 3, step 7 and Fig. 2e). The final upper and lower boundary coordinates were then saved. In the following, the upper boundary of the diaphragmatic motion diagram (see also Fig. 2f, step 8) was then used to estimate the excursion (as documented by [8]), cycle duration, inspiration time, total time, slope, relaxation rate, steepest slope and MRR_SAUS (see Fig. 2f and Fig. 3, step 8). Two additional methods for estimating the upper and lower boundaries of the diaphragm

TABLE 1. Manual (MRR_MUS), manual biopac® (MRR_MB) and Semi-automated (MRR_SAUS) measurements of the diaphragmatic motion.

	Diaphragmatic Features	NRES (N=20)				RES (N=7)			
		Mean±std	Median (IQR)	%SEM	%MAE	Mean±std	Median (IQR)	%SEM	%MAE
SAUS	Cycle duration [sec]	2.10±0.13	1.97(0.33)	1.43	1.0	2.02±0.16	2.0(1.2)	2.99	0.8
SAUS	Excursion [mm]	12.11±0.93	11.4(5.67)	1.71	5.3	13.34±1.52	11.99(7.6)	4.30	1.64
SAUS	Inspiration time [sec]	0.85±0.11	0.81(0.45)	3.02	2.0	0.86±0.13	0.82(0.47)	5.66	0.7
SAUS	Slope (Exc/Insp.time) [mm/sec]	15.3±2.5	15.0(8.94)	3.8	6.9	18.5±4.2	17.8(16)	8.57	0.7
SAUS	Relaxation time [sec]	1.26±0.02	1.11(0.67)	3.6	2.0	1.16±0.03	1.1(0.8)	1.01	0.6
SAUS	Relaxation rate (Exc/Relax.time) [mm/sec]	11.0±2.3	10.0(5.6)	4.7	4.2	13.2±5.3	12.2(8.8)	15.10	2.6
	MRR_MUS [1/sec]	2.36±1.19	2.33(2.1)	11.6	1.56	5.8±2.10	2.1(1.69)	11.9	2.51
	MRR_MB [1/sec]	3.93±0.89	3.86(1.47)	5.2	-	3.73±0.52	3.81(0.76)	5.65	-
	MRR_SAUS [1/sec]	3.94±0.91	3.56(1.4)	5.3	1.56	4.98±1.98	3.72(1.73)	6.31	2.18
SAUS	Steepest slope [mm/sec]	54.68±10.58	49.4(37.5)	4.33	-	74.22±4.99	71(49)	6.13	-
SAUS	Y-distance [mm]	13.79±1.17	12.4(8.67)	1.90	-	15.14±0.97	13(9.5)	1.86	-

NRES: ultrasound M-mode images without the use of resistance during breathing; RES: ultrasound M-mode images with the use of resistance during breathing; MUS, MB, SAUS: Manual, manual Biopac® and semi-automated, ultrasound measurements; %SEM: Standard error of the mean*100; %MAE: Percentage of the mean absolute error. The comparisons for extracting the errors were made between the MUS and the SAUS measurements.

were additionally tested in this work and compared with the one proposed. The first one was based on a simple pixel differencing for edge detection and the second one on an edge detection method based on isocontour geometry included in the Matlab® image processing toolbox. The best performed method, which was the one based on the simple pixel differencing for edge detection was then used to generate the results shown in Table 1.

D. ESTIMATION OF THE MRR_SAUS

The MRR_SAUS can be found by estimating the steepest slope of the descending section on the diaphragmatic displacement curve [6]. The y-axis distance of each descending section was found as shown in Fig. 2f. Each descending section of the diaphragmatic graph from the maximum point (end of the diaphragmatic contraction) up to the minimum point (end of the diaphragmatic relaxation), was divided into 10 equidistant segments (see Fig. 2f and Fig. 3). In each part of the descending section, two edge points A (x_1, y_1) and B (x_2, y_2) were taken at a time, in order to estimate the slope of the segment under investigation, which was given with:

$$slope = \frac{y_2 - y_1}{(x_2 - x_1)} \tag{3}$$

Thus, the maximum slope from each descending section in the diaphragmatic displacement diagram was estimated and marked with a thicker line (see Fig. 2f). The y-axis distance is the distance between the maximum and minimum points of the descending section. The estimation of the MRR can thus be calculated as (see also Fig. 2f):

$$MRR\_SAUS = \frac{steepest\ slope\ value}{y\ axis\ distance} \tag{4}$$

Finally, the average MRR_SAUS from all descending sections of the diaphragmatic curve was calculated and presented to the user. It is understood that in order to calculate the steepest slope of the diaphragmatic displacement all breaths illustrated on the M-mode ultrasound image must be included within the selected ROI as shown in Fig. 2a) (see also Fig. 3, step 9).

E. EVALUATION METRICS

For quantitatively evaluating the proposed method the following evaluation metrics were computed (see Fig. 3, step 10):

1) THE MEAN ABSOLUTE (%) ERROR (MAE)

$$MAE = \frac{1}{N}\sum_{i}^{N}\left|\frac{A_i - M_i}{M_i}\right| * 100 \tag{5}$$

where i, represents the breath number, M_i and A_i indicate the manual and semi-automated measurements respectively and N is the number of breaths.

2) THE STANDARD ERROR OF THE MEAN (SEM)

$$SEM\%\,(x) = \left[\frac{\frac{std(x)}{\sqrt{N}}}{mean\,(x)}\right] * 100 \tag{6}$$

where x represents the current measurement of the diaphragmatic feature and N the number of breaths measured.

F. STATISTICAL ANALYSIS

In order to further evaluate the proposed method, the Wilcoxon rank sum test [16], was used in order to identify if for each set of measurements, a significance

IEEE Journal of Translational Engineering in Health and Medicine

TABLE 2. Comparison between manual (mus), manual biopac®(mb) and semi-automated (saus) Mean measurements of the MRR based on the Wilcoxon rank sum test for the nres and res groups.

	NRES_MRR_MUS	RES_MRR_MUS	NRES_MRR_MB	RES_MRR_MB
NRES_MRR_SAUS	S (p=0.0001) ρ=0.79 (p=0.01)		NS (p=0.62) ρ=0.96 (p=0.001)	
RES_MRR_SAUS		S (p=0.02) ρ=0.88 (p=0.01)		NS (p=0.58) ρ=0.83 (p=0.02)
NRES_MRR_MB	S(p=0.001) ρ=0.81 (p=0.001)			
RES_MRR_MB		NS(p=0.3) ρ=0.77 (p=0.05)		

MUS, MB, SAUS: Manual, manual Biopac® and automated, ultrasound measurements; SD: Significantly different at p<0.05, NS: non-statistical significant different at p≥0.05; ρ: Spearman correlation coefficient; NS, S: Non-significantly statistically different at p≧0.05, significantly statistically different at p<0.05.

difference (SD) or not (NSD) exists between the two different groups investigated (NRES, RES). For significance difference, we require $p < 0.05$. This was done for each set of measurements for independent samples of same sizes with a confidence level of 95%. Furthermore, box plots for the three different groups and for all different measurements were plotted. Bland-Altman plots with 95% confidence intervals, were also used to further evaluate the agreement between the manual (MUS, MB) and the semi-automated (SAUS) measurements.

III. RESULTS

Table 1 tabulates the results of the manual and semi-automated measurements for the NRES and RES groups investigated in this study for an average of 8 breathing cycles. The mean ± std and median (inter quartile range (IQR)) measurements of the cycle duration, excursion, inspiration time, slope, relaxation time, relaxation rate and MRR were computed. Furthermore, the percentage standard error of the mean (%SEM) and the percentage of mean absolute error (%MAE) were computed. As shown in Table 1, we computed the semi-automated ultrasound MRR measurements on all NRES/RES images, using the proposed system (MRR_SAUS = 3.94 ± 0.91/4.98 ± 1.98 [1/sec], %SEM = 5.3/6.31), and compared them with the manual measurements made by a clinical expert (MRR_MUS = 2.36 ± 1.19/5.8 ± 2.1 [1/sec], %SEM = 11.6/11.9 [1/sec]) and those made by a reference manual method (MRR_MB = 3.93 ± 0.89/3.73 ± 0.52 [1/sec], %SEM = 5.2/5.65), performed manually with the Biopac®system.

Figure 4 illustrates the Bland-Altman plot between the reference manual Biopac®system (MRR_MB) and the semi-automated (MRR_SAUS) measurements of the MRR for the NRES (indicated with circles in Fig. 4, N = 20) and the RES (indicated with empty rectangles in Fig. 4, N = 7) cases investigated in this study. The difference of the two methods for all measurements investigated (Biopac®semi-automated vs manual) were 0.6 + 3.6 [1/sec] and 0.6-2.3 [1/sec] with a Spearman correlation of $\rho = 0.20$ (p = 0.15) and a non-statistical significance difference (NS at p = 0.85) using the Wilcoxon rank sum test. It was shown that the outliers belong entirely to the RES group.

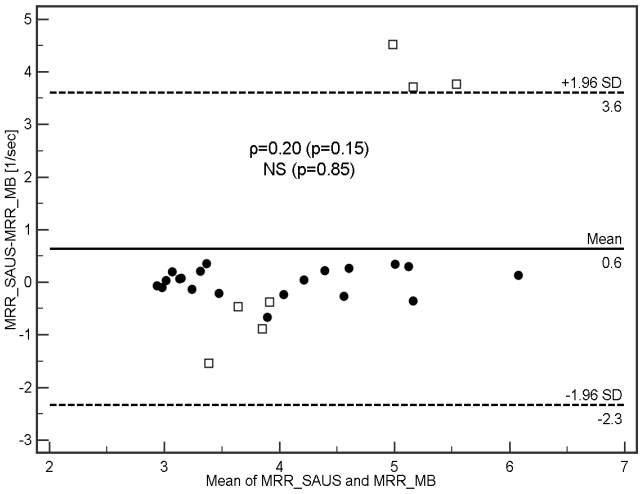

FIGURE 4. Bland-Altman plot illustrating the agreement between the Biopac®MRR manual (MRR_MB) and the MRR semi-automated measurements (MRR_SAUS) for the MRR index on the NRES (N = 20, indicated with circles) and the RES (N = 7, indicated with empty rectangles) ultrasound M-mode images of the diaphragmatic muscle investigated in this study. Correlation: $\rho = 0.20$ at p = 0.15 (F-ratio = 2.26, Regression equation: MRR_SAUS = 2.35-0.48 ∗ MRR_MB). Non-significantly different (NS) at p = 0.28, using Wilcoxon rank-sum test (see also Table 2).

In Fig. 5 we illustrate box plots for all images (NRES in the left part and RES in the right part of Fig. 5) and the three different groups (MUS, MB, SAUS) investigated in this study for the MRR measurements.

In Table 2 we present a comparison based on the Wilcoxon rank sum test between the manual (MB and MUS) and SAUS measurements of the MRR for all cases investigated. MRR_SAUS and MRR_MB measurements were not statistically significantly different for NRES and RES subjects (p = 0.62/p = 0.58) with a good correlation ($\rho = 0.96/\rho = 0.83$) but were significantly different with the MRR_MUS measurements made by the clinical expert. It should be furthermore noted that the refence method for measuring the MRR is the MRR_MB [6], which has been found in this study to be non-statistically significantly different with the proposed semi-automated method (MRR_SAUS).

The proposed system in this work maybe therefore used in clinical practice with confidence as the proposed system

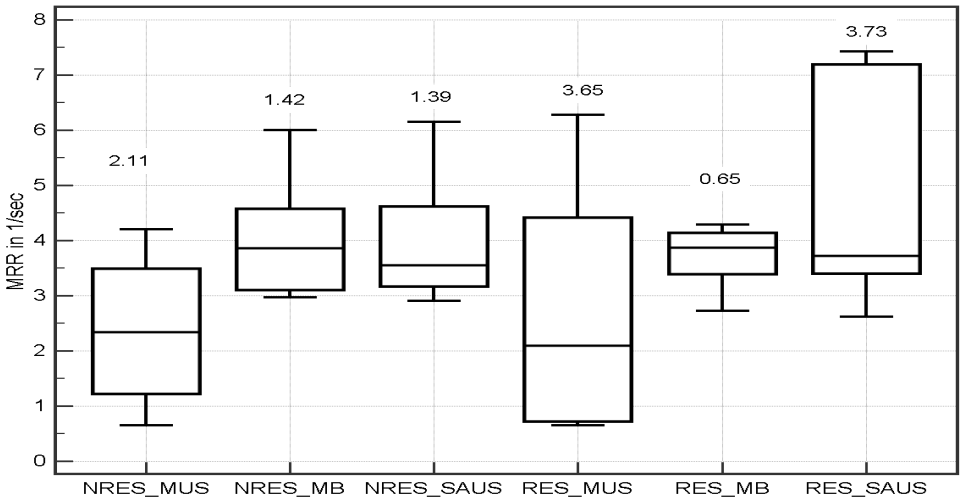

FIGURE 5. Box plots for the MRR index for the NRES (left part) and RES (right part) groups. The interquartile range (IQR) is shown above each box plot.

agrees with the manual measurements of the Biopac® reference system.

IV. DISCUSSION

The objective of this study was to develop and evaluate a semi-automated system for the measurement of the diaphragmatic motion and the estimation of the MRR_SAUS index from ultrasound M-mode images of the diaphragmatic muscle. It is well documented that diaphragmatic thickness, which is used to identify diaphragmatic atrophy is not always a reliable measure in all clinical settings. Measurements of thickness for instance may miss an acutely paralyzed diaphragm (abnormal thickness: 1.3-1.9 mm vs normal thickness: 2.2-2.8 mm) and could incorrectly identify atrophy in a low weight individual with a healthy, yet thin, diaphragm [17], [18]. Therefore, additional metrics such as the one proposed in this study (MRR_SAUS) are required for reliably following the diaphragmatic function. It should be furthermore noted that this is the first study presented in the literature (with the exception of [10], performed by our group), where MRR is computed automatically from ultrasound M-mode images of the diaphragmatic muscle.

Furthermore, as also shown in Table 1 and Fig. 4, the MRR_SAUS error between the manual and the semi-automated measurements on all the NRES/RES images were small (%SEM = 5.3/6.31, %MAE = 1.56/2.18). The difference between the manual (MRR_MB) and the semi-automated (MRR_SAUS) measurements were also very small as shown in Fig. 4. Figure 5 also shows that the distribution of the semi-automated MRR measurements (SAUS), specifically for the NRES is more robust with lower IQR values when compared with the MUS and MB methods. The semi-automated MRR measurements (MRR_SAUS) estimated with the proposed system can thus be used in the clinical practice with confidence as the proposed system agrees with the reference method (MB). It is furthermore shown from Fig. 4 and Table 1, that the proposed method overestimates the MRR_SAUS measurements (by 0.3 1/sec, see also Fig. 4) when compared with the MRR_MB. It was also shown from Table 1 that the manual and the automated MRR values were higher for the RES subjects when compared with the NRES subjects with statistically significant differences between them (see also Table 2).

Matamis *et al.* [6], studied the use of ultrasonography for the evaluation of diaphragmatic function in ICU patients. It was shown that the value of the diaphragmatic excursion manually estimated, in healthy male individuals was 18 ± 3 mm and that ultrasonography can non-invasively assist on the evaluation of the diaphragmatic muscle in post-operative patients as also reported in [8]. It was also reported in [4]–[6], that the golden method for measuring the MRR is the MRR_MB, which was performed by the Biopac®system. As shown in Table 2 non-statistical significant differences were found between the method proposed in this work (MRR_SAUS) and the MRR_MB.

In another study [25], M-mode sonography was used to manually assess diaphragmatic motion in 40 healthy volunteers breathing under conditions of inspiratory resistive loading. It was shown that inspiratory resistive loading induced significant changes in the diaphragmatic contraction pattern, which mainly consisted of decreased velocity of diaphragmatic displacement with no change in diaphragmatic excursion. The slope of the diaphragmatic contraction in subjects with breathing problems, during quiet breathing, was 13 ± 0.4 mm/s [25]. A protocol was also suggested in [18] for evaluating ultrasonography in the study of the diaphragmatic motion.

M-mode images of 40 healthy subjects were investigated in [26]. The resting and forced diaphragmatic excursions were 18.4 ± 7.6 mm and 78.8 ± 13.3 mm, respectively, unrelated to demographic or anthropometric parameters.

IEEE Journal of Translational Engineering in Health and Medicine

Gerscovitch *et al.* [19], investigated diaphragmatic paralysis on 102 subjects using ultrasound M-mode imaging and manual measurements. It was found that women demonstrated greater diaphragmatic excursion values than men (15.4 mm for women vs 13.9 mm for men). Also, differences were found between the left and right hemidiaphragm. Slightly lower values were also found for the diaphragmatic excursion in the present study.

The effects of stroke on diaphragmatic motion using M-mode ultrasound images were investigated in [7] and correlated with pulmonary function in hemiplegic patients (10 normal versus 10 stroke subjects). Among healthy subjects, men (24.3 ± 5.1 mm) had greater diaphragmatic excursion than women (23.7 ± 6.6 mm). For the stroke subjects, a reduction in the excursion was observed for both men and women (15.9 ± 3.7 mm). There was also a statistically significant difference estimated for the excursion between normal and stroke subjects ($p < 0.01$).

In the largest study found in the literature [8], manual readings of the diaphragmatic excursion from 236 healthy subjects were taken in quiet breathing by two experts from M-mode images. During deep breathing, an obscuration of the diaphragm by the descending lung was noted in subjects with marked diaphragmatic excursion. The lower normal limit values of the diaphragmatic excursion were close to 9 mm for women and 10 mm for men during quiet breathing, 16 mm for women and 18 mm for men during voluntary sniffing and 37 mm for women and 47 mm for men during deep breathing.

In [20], an investigation of the diaphragmatic dysfunction was presented using M-mode ultrasonography in 88 ICU patients. It was found that the excursion, assessed manually, was below 10 mm. It was furthermore shown that ultrasonography of the diaphragm may be useful in identifying patients at high risk of difficult weaning.

Furthermore, in [21], the usefulness of ultrasonography in manually detecting diaphragmatic dysfunction as a cause of acute respiratory failure with a subsequent change in patient management was for the first time demonstrated. It was also shown in [22] that ultrasound measures of diaphragm muscle thickening taken form 63 mechanically ventilated patients, may predict extubation success or failure with pressure support and spontaneous breathing weaning trials. It was also shown that this method may be especially helpful in reducing the number of failed extubations. Similarly, in [23], it was shown that the assessment of the diaphragm thickening fraction investigated on 46 subjects, may perform similarly to other weaning indexes.

The diaphragmatic movement (inspiration, expiration and excursion) of 14 asymptomatic adults (9 males, 5 females; mean age $= 28.4 \pm 3.0$ years) was investigated in [24]. Strong correlations (ranging from 0.78 to 0.83), between ultrasound and radiographic manual imaging measurements of the diaphragm during inhalation, exhalation, and excursion were found.

Finally, in [11], simulated videos of the diaphragmatic motion in healthy subjects were used to report an excursion of 17.73 ± 1.01 mm (SEM $= 3.28\%$), in contrast with 18.31 ± 0.0 mm, which was reported in our study (SEM $= 0.00\%$ and MAE $= 0.03$) on M-mode images. Furthermore, findings in [11], showed that in real ultrasound videos of the abnormal diaphragm the diaphragmatic displacement was 9.47 ± 0.23 mm.

In all of the above studies, the assessment and the evaluation of the diaphragm was performed manually by experts, which includes intra- and inter-observer variability. A major difficulty that a clinical expert faces when calculating a patient's MRR, is to identify the exact location of the steepest part of the diaphragmatic displacement waveform. The expert is required to identify that part of the curve, where the slope of the diaphragmatic displacement should be ideally calculated (see also Fig. 2f). This involves high intra- and inter-observer variabilities, which may produce different results. The semi-automated analysis system for measuring the diaphragmatic motion and estimating the maximum relaxation rate proposed in this work, partially overcomes this problem, since, due to digital processing of the ultrasound diaphragmatic images, identification of the right points to draw the slope line becomes easier and more accurate.

The inclusion of the resistive device in the breathing system was not aiming to induce fatigue or mimic any specific clinical cases, but to simply induce a change in breathing conditions. We subsequently examined if the relationship between the MRR_SAUS, MRR_MUS and MRR_MB that we found during normal breathing remained the same during resistive breathing, despite the change in the ventilatory setting. It is noted that the performance of MRR_SAUS is similar for both NRES and RES subjects. There was no significant difference between NRES_MRR_SAUS and NRES_MRR_MB as well as between RES_MRR_SAUS and RES_MRR_MB as documented in Table 2. In addition, it is noted that %SEM and %MAE for the NRES cases were slightly lower than the RES cases as documented in Table 1.

To the best of our knowledge, there are no other studies reported in the literature, where the value of the ultrasonic diaphragmatic MRR was estimated either semi-automatically or automatically. Additional research is required in a larger number of images by employing additional evaluation metrics and observers for further investigating the use of the proposed MRR_SAUS index in the assessment of the diaphragmatic motion.

A. LIMITATIONS

There are also some limitations for the present study, which are summarized below. Ultrasound is operator dependent, suffering from intra- and inter-observer variabilities [14], [15], [18] specifically in diaphragm assessment as also documented in [1], [8], [18], and [20]. Bad visualization of the left hemi-diaphragm was reported in the past [1], [2], with an incidence of failure to visualize between 28–63%. However, more recently, bad visualization was significantly

improved using a subcostal approach and correct positioning [8], [19]. The measurement of excursion depends on maximal voluntary inspiration effort. This limits the interpretation and generalization of cut-off values of excursion amplitude measurement in heterogeneous populations [27].

A further limitation of this study could be the small size of the images, especially for the NRES (N = 7), on which the method was applied. It was documented in [28], that measuring parameters of the diaphragmatic displacement, slope and time from an M-mode diaphragmatic excursion waveform has long been practiced. The manual measurements basically consist of measurement of characteristics of the diaphragmatic displacement waveform once the examiner has decided which part of the curve will be assessed. These parameters carry an excellent intra- and inter-observer reproducibility, limiting, therefore, the number of observers and images necessary for reliable interpretation of the results. Moreover, despite the relatively small number of RES and NRES samples, each image usually contains at least 5-8 breaths, increasing, therefore, the number of available breaths for assessment and measurement.

Another limitation to the widespread use of ultrasound for diaphragm assessment is a lack of reference values for diaphragmatic parameters [18]. This is because different groups have used different ranges of lung volumes for quiet breathing, deep breathing, or sniff maneuvers. Depending on the body position, weight, height, or physical condition of the subject, the upper rib cage and neck muscles were shown to make a greater contribution to inspired volume in certain subjects [1]. Ultrasound parameters of thickness and excursion can also vary depending on the initial point of measurement by the end of the expiration [1], [17] or the beginning of the inspiration [29]. It is therefore recommended, when normative data are collected, simultaneous spirometric measurements to be performed [8], [20].

B. FUTURE DIRECTIONS

Future research on diaphragmatic ultrasound analysis could further evaluate the relationship between diaphragmatic displacement, thickness and MRR index and compare these parameters with additional evaluation metrics for evaluating the diaphragmatic strength for improving ventilator trigger delay and synchrony. Furthermore, to utilize the findings of this study to follow diaphragmatic atrophy or recovery from atrophy in patients suffering from critical illness polyneuromyopathy or assess diaphragmatic function in patients during prolonged or difficult weaning from mechanical ventilation. Additionally, standardized protocols for the ultrasound assessment of the diaphragm should be designed including information relating the MRR_SAUS index and the diaphragmatic excursion. Reference values for the diaphragm thickness, excursion, amplitude, velocity and the MRR_SAUS index should also be established as well as a relation between them could be found. The method proposed in this work offers a non-invasive tool to calculate diaphragmatic MRR, a parameter with clinical implications in weaning from mechanical ventilation. However, the traditional measurement of MRR is accomplished using an invasive and cumbersome technique, resulting in the restriction of this potentially helpful parameter mainly in the laboratory. In this study, we propose a non-invasive method to calculate MRR, which, in combination with the rapidly increasing familiarity with the use of diaphragmatic ultrasound, can restore the use of MRR as a valuable parameter in clinical ICU practice.

V. CONCLUDING REMARKS

It is shown in this study that the MRR_SAUS measurements extracted from an M-mode ultrasound diaphragmatic image may be used successfully for measuring diaphragmatic weakness or paralysis (normality or abnormality).

Slowing of the MRR when the ventilatory conditions change indicates diaphragmatic fatigue with possible subsequent difficulty in disconnecting the ventilator. However, the results of this study should be examined further and validated on a larger number of subjects, so that concrete conclusions can be drawn for the use of the MRR_SAUS as a validated measure for the normal diaphragmatic motion. Future work will investigate the possible incorporation of the proposed system into a computer aided diagnostic system that supports diaphragmatic motion image and video analysis, providing an automated system for the early diagnosis of the diaphragmatic dysfunction.

REFERENCES

[1] J. L. Wait and R. L. Johnson, "Patterns of shortening and thickening of the human diaphragm," *J. Appl. Physiol.*, vol. 83, no. 4, pp. 1123–1132, 1997.
[2] J. F. Murray, "Ventilation," in *The Normal Lung*, 2nd ed. London, U.K.: Saunders, 1986, pp. 83–119.
[3] D. V. Bates, *Respiratory Function in Disease*, 3rd ed. London, U.K.: Saunders, 1989, pp. 197–201.
[4] J. C. Goldstone, M. Green, and J. Moxham, "Maximum relaxation rate of the diaphragm during weaning from mechanical ventilation," *Thorax*, vol. 49, no. 1, pp. 54–60, 1994.
[5] S. A. Esau, F. Bellemare, A. Grassino, S. Permutt, C. Roussos, and R. L. Prady, "Changes in relaxation rate with diaphragmatic fatigue in humans," *J. Appl. Physiol.*, vol. 54, no. 5, pp. 1353–1360, 1983.
[6] D. Matamis *et al.*, "Sonographic evaluation of the diaphragm in critically ill patients. Technique and clinical applications," *Intensive Care Med.*, vol. 39, no. 5, pp. 801–810, 2013.
[7] K.-J. Jung, J.-Y. Park, D.-W. Hwang, J.-H. Kim, and J.-H. Kim, "Ultrasonographic diaphragmatic motion analysis and its correlation with pulmonary function in hemiplegic stroke patients," *Ann. Rehabil. Med.*, vol. 38, no. 1, pp. 29–37, 2014.
[8] A. Boussuges, Y. Gole, and P. Blanc, "Diaphragmatic motion studied by m-mode ultrasonography: Methods, reproducibility, and normal values," *Chest*, vol. 135, no. 2, pp. 391–400, 2009.
[9] M. Cassart, N. Pettiaux, P. A. Gevenois, M. Paiva, and M. Estenne, "Effect of chronic hyperinflation on diaphragm length and surface area," *Amer. J. Respiratory Crit. Care Med.*, vol. 156, no. 2, pp. 504–508, 1997.
[10] C. D. Loizou, C. P. Loizou, D. Matamis, K. Soleimezi, G. Minas, and C. S. Pattichis, "Suggesting a sonographic index to measure ultrasound diaphragmatic MRR," in *Proc. 14th Mediter. Conf. Med. Biol. Eng. Comput.*, Paphos, Cyprus, vol. 57, Mar./Apr. 2016, pp. 355–360.
[11] C. Chrysostomou, C. P. Loizou, G. Minas, K. Delimbasis, and C. S. Pattichis, "Measurement of ultrasonic diaphragmatic motion," in *Proc. 37th Int. Conf. IEEE Eng. Med. Biol. Soc.*, Milan, Italy, Aug. 2015, pp. 6358–6361.
[12] T. Elatrozy, A. N. Nicolaides, T. Tegos, A. Zarka, M. Griffin, and M. Sabetai, "The effect of B-mode ultrasonic image standardisation on the echodensity of symptomatic and asymptomatic carotid bifurcation plaques," *Int. Angiol.*, vol. 17, no. 3, pp. 179–186, 1998.

IEEE Journal of Translational Engineering in Health and Medicine

[13] C. P. Loizou, C. S. Pattichis, C. I. Christodoulou, R. S. H. Istepanian, M. Pantziaris, and A. Nicolaides, "Comparative evaluation of despeckle filtering in ultrasound imaging of the carotid artery," *IEEE Trans. Ultrason., Ferroelectr., Freq. Control*, vol. 52, no. 10, pp. 1653–1669, Oct. 2005.

[14] C. P. Loizou and C. S. Pattichis, *Despeckle Filtering for Ultrasound Imaging and Video: Algorithms and Software* (Synthesis Lectures on Algorithms and Software in Engineering), vol. 7, no. 1. San Rafael, CA, USA: Morgan & Claypool, 2015, pp. 1–180.

[15] C. P. Loizou, C. S. Pattichis, M. Pantziaris, T. Tyllis, and A. Nicolaides, "Snakes based segmentation of the common carotid artery intima media," *Med. Biol. Eng. Comput.*, vol. 45, no. 1, pp. 35–49, 2007.

[16] M. P. Fay and M. A. Proschan, "Wilcoxon-Mann-Whitney or t-test? On assumptions for hypothesis tests and multiple interpretations of decision rules," *Stat. Surv.*, vol. 4, pp. 1–39, Apr. 2010.

[17] E. M. Summerhill, Y. A. El-Sameed, T. J. Glidden, and F. D. McCool, "Monitoring recovery from diaphragm paralysis with ultrasound," *Chest*, vol. 133, no. 3, pp. 737–743, 2008.

[18] A. Sarwal, F. O. Walker, and M. S. Cartwright, "Neuromuscular ultrasound for evaluation of the diaphragm," *Muscle Nerve*, vol. 47, no. 3, pp. 319–329, 2013.

[19] E. O. Gerscovich, M. Cronan, J. P. McGahan, K. Jain, C. D. Jones, and C. McDonald, "Ultrasonographic evaluation of diaphragmatic motion," *J. Ultrasound Med.*, vol. 20, no. 6, pp. 597–604, 2001.

[20] W. Y. Kim, H. J. Suh, S. B. Hong, Y. Koh, and C. M. Lim, "Diaphragm dysfunction assessed by ultrasonography: Influence on weaning from mechanical ventilation," *Crit. Care Med.*, vol. 39, no. 12, pp. 2627–2630, 2011.

[21] F. Barbariol, L. Vetrugno, L. Pombei, A. D. Flaviis, and G. D. Rocca, "Point-of-care ultrasound of the diaphragm in a liver transplant patient with acute respiratory failure," *Crit. Ultrasound J.*, vol. 7, no. 1, pp. 1–4, 2015.

[22] E. DiNino, E. J. Gartman, J. M. Sethi, and F. D. McCool, "Diaphragm ultrasound as a predictor of successful extubation from mechanical ventilation," *Thorax*, vol. 69, pp. 423–427, May 2014.

[23] G. Ferrari, G. De Filippi, F. Elia, F. Panero, G. Volpicelli, and F. Aprá, "Diaphragm ultrasound as a new index of discontinuation from mechanical ventilation," *Crit. Ultrasound J.*, vol. 6, no. 1, p. 8, 2014.

[24] D. K. Noh, J. J. Lee, and J. H. You, "Diaphragm breathing movement measurement using ultrasound and radiographic imaging: A concurrent validity," *Bio-Med. Mater. Eng.*, vol. 24, pp. 947–952, Jan. 2014.

[25] E. Soilemezi *et al.*, "Sonographic assessment of changes in diaphragmatic kinetics induced by inspiratory resistive loading," *Respirology*, vol. 18, no. 3, pp. 468–473, 2013.

[26] A. Testa, G. Soldati, R. Giannuzzi, S. Berardi, G. Portale, and N. S. Gentiloni, "Ultrasound M-mode assessment of diaphragmatic kinetics by anterior transverse scanning in healthy subjects," *Ultrasound Med. Biol.*, vol. 37, no. 1, pp. 44–52, 2011.

[27] N. Lerolle and J.-L. Diehl, "Ultrasonographic evaluation of diaphragmatic function," *Crit. Care Med.*, vol. 39, no. 12, pp. 2760–2761, 2011.

[28] E. Vivier *et al.*, "Diaphragm ultrasonography to estimate the work of breathing during non-invasive ventilation," *Intensive Care Med.*, vol. 38, no. 5, pp. 796–803, 2012.

[29] F. Kantarci *et al.*, "Normal diaphragmatic motion and the effects of body composition: Determination with M-mode sonography," *J. Ultrasound Med.*, vol. 23, no. 22, pp. 255–260, 2004.